Macroscopic Magnetic Islands and Plasma Energy Transport

F. Porcelli,[1] E. Rossi,[1] G. Cima,[2] and A. Wootton[3]
[1]*Istituto Nazionale Fisica della Materia and Department of Energetics, Politecnico di Torino, 10129 Torino, Italy*
[2]*Fusion Research Center, University of Texas at Austin, Austin, Texas 78712*
[3]*Lawrence Livermore National Laboratory, Livermore, California 94551*
(Received 30 September 1998)

A model is presented based on the combined effects of $m/n = 1$ magnetic island dynamics, localized heat sources, large heat diffusivity along magnetic field lines, and plasma rotation, which may explain the multipeaked temperature profiles and transport barriers observed in tokamak plasmas heated by electron-cyclotron-resonant waves. [S0031-9007(99)08455-0]

PACS numbers: 52.50.Gj, 52.30.Jb, 52.35.Py, 52.55.Fa

Experiments in magnetically confined, high temperature plasmas heated by intense electromagnetic waves at the electron-cyclotron-resonance frequency have revealed peculiar and hitherto unexplained plasma behavior. The most striking results [1] come from the Rijnhuizen Tokamak Project (RTP), where electron cyclotron heating (ECH) with maximum power $P \approx 360$ kW is applied to the toroidal plasma. In this experiment, a double-pulse multiposition Thomson scattering diagnostic measures the electron temperature profile with a very high spatial resolution. In the plasma central region, the measured electron temperature profiles exhibit several peaks, which have led the RTP group to suggest a "filamentary" structure. In addition, ECH experiments in RTP [2] have revealed very sharp temperature gradients just outside the sawtooth mixing radius. Other minor structures in the T_e profiles are sometimes observed near rational surfaces with $q > 1$. The sharp gradients at the sawtooth mixing radius, as well as the other minor structures, have been interpreted as due to the presence of "transport barriers" on rational q surfaces [1–3].

The RTP results have raised the question whether the observed peculiar behavior is specific to ECH or whether it is in fact universal to all tokamak plasmas. Clearly, an answer to this question relies on our understanding of the underlying magnetic structure. It must be emphasized that this structure in the plasma central region is strongly affected by the so-called sawtooth relaxation oscillations [4], associated with the instability of a resistive kink mode with toroidal $n = 1$ and dominant poloidal $m = 1$ mode numbers, which results in a periodically growing $m/n = 1$ magnetic island.

In this Letter, we concentrate on results from the Texas Experimental Tokamak Upgrade (TEXT-U) [5], which strongly suggest that the observed temperature behavior is the outcome of an interplay between sawteeth and ECH. The objective is to clarify this interplay from a theoretical standpoint. We present a model for the evolution of the electron temperature profiles, based on the following essential ingredients: (i) a reconstruction of magnetic surfaces based on the sawtooth reconnection process; (ii) the presence of a localized electron heat source; (iii) the effect of plasma rotation; (iv) the effect of anisotropic heat diffusion, whereby the parallel (along the field lines) heat diffusion coefficient, $\chi_\parallel$, is taken as very large, and the perpendicular coefficient, $\chi_\perp$, as relatively small, on the sawtooth period time scale and spatial extent. This model is able to reproduce qualitatively the observed features of the TEXT-U and RTP temperature profiles, in particular, sharp gradients at the sawtooth mixing radius and several peaks, even when a strictly constant $\chi_\perp$ profile is assumed. What is special with ECH, in contrast with other heating schemes, is that electron cyclotron waves transfer their energy directly to the electrons, with no delay and in a very localized deposition region [6].

Let us first summarize the relevant results from TEXT-U [5]. The main tokamak parameters are $R = 1.05$ m, $a = 0.27$ m, $B \approx 2$ T, $I_p \approx 230$ kA, and central electron density $n_e \approx 3.0 \times 10^{19}$ m^{-3}. The experiment is equipped with an ECH system which delivers a maximum power $P \approx 270$ kW. The electron temperature is measured by an electron cyclotron emission (ECE) diagnostic. The typical spatial resolution of the ECE signal [5] is below 1 cm, which is not as good as the Thompson scattering system on RTP. On the other hand, the ECE diagnostic on TEXT-U has a very high temporal resolution, $O(20\ \mu\text{s})$, over an extended time interval. In this sense, the temperature measurements on TEXT-U can be considered as complementary to those on RTP.

Figure 1 shows an example of the central electron temperature evolution in TEXT-U. Shown in Fig. 1(a) are nearly three sawtooth ramps, with a period $\tau_{\text{saw}} \approx 2$ ms and with fast oscillations superimposed. The period of the fast oscillations matches the plasma toroidal rotation period, $\tau_{\text{rot}} \approx 160\ \mu$s in this case. If these oscillations are indeed due to the presence of an $m/n = 1$ magnetic island, then this island is formed early on during each sawtooth ramp and maintains a nearly saturated amplitude for most of the ramp. Figure 1(b) presents an example of an ECE T_e profile; a sequence of these profiles can be found in Fig. 10 of Ref. [5]. The profiles at time

 0031-9007/99/82(7)/1458(4)$15.00

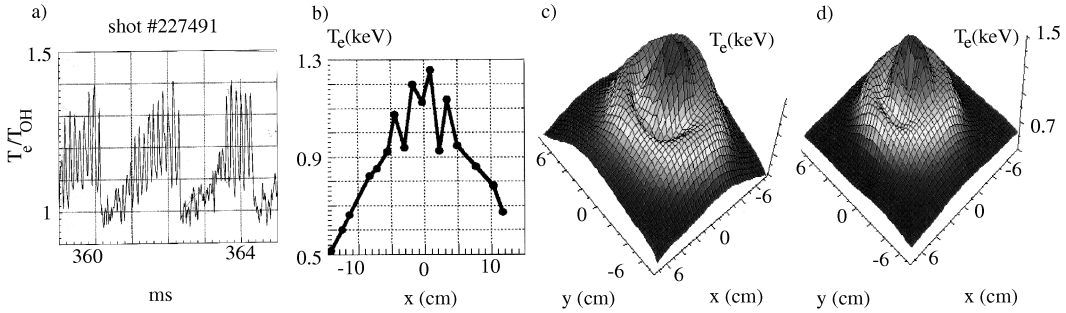

FIG. 1. Electron temperature in TEXT-U. (a) Central T_e evolution; (b) an example of T_e profiles; (c) and (d): 3D reconstructions.

intervals $t_2 - t_1 \approx \tau_{\rm rot}$ nearly coincide, which confirms that we are indeed observing a toroidal $n = 1$ structure. These profiles exhibit four to five peaks and are similar to the filamentlike temperature structures previously reported in RTP. However, the RTP observations lack time history. With the temporal and spatial resolution available on TEXT-U, we find that the structures are cyclic and consistent with a fixed structure in the rotating plasma frame. The main poloidal $m = 1$ structure can be deduced from 3D reconstructions of the type shown in Figs. 1(c) and 1(d), where the time variable has been transformed into the poloidal angle variable under the assumption of rigid rotation.

Let us now present our theoretical model. We assume, for simplicity, a "rectified" tokamak, i.e., a cylindrical plasma column of length L with periodic boundary conditions. In the absence of an $m = 1$ island, magnetic surface cross sections are concentric circles of constant normalized helical flux, $\psi_{*\rm in}(r) = \int_0^{r^2} [q_{\rm in}(x)^{-1} - 1]\, dx$, where the subscript "in" stands for "initial," i.e., before the island formation. For a typical (i.e., monotonic) $q_{\rm in}(r)$ profile, $\psi_{*\rm in}(r)$ has a maximum at the $q_{\rm in} = 1$ radius, $r = r_s$. The growth of an $m = 1$ island is brought about by a rigid shift of surfaces within the original $q_{\rm in} = 1$ surface. The helical flux, $\psi_*(r, \alpha; t)$, where $\alpha = \theta - 2\pi z/L$, remains nearly constant on moving fluid elements. At each stage of the reconnection process, the island separatrix is formed by two circles of radii $r_{1sp} < r_s$ and $r_{2sp} > r_s$, where $\psi_{*\rm in}(r_{1sp}) = \psi_{*\rm in}(r_{2sp})$, with the center of the inner circle (i.e., the original magnetic axis) displaced from its initial position by a distance $\xi(t) = r_{2sp} - r_{1sp}$ (see Fig. 2). In addition, toroidal flux conservation is assumed; with $B_z \approx$ const, this is equivalent to area conservation; i.e., when the island separatrix later evolves into a croissant-shaped surface, the area encircled in the poloidal plane by this surface is constant and equal to $A = \pi(r_{2sp}^2 - r_{1sp}^2)$. The contour of the croissant is also a surface of constant helical flux, specifically $\psi_*(r, \alpha; \xi) = \psi_{*\rm in}(r_{1sp})$. This model for the $m/n = 1$ island evolution is based on the specific convection pattern associated with the resistive internal kink mode [7] and on the ideal MHD assumption of frozen magnetic flux through moving fluid elements, approximately valid everywhere except in the immediate neighborhood of the island X-point and current sheet.

The well known Kadomtsev model [8] for the sawtooth relaxation corresponds to the two basic reconnection rules described above and to the following assertions: (i) The reconnection process proceeds until full reconnection, i.e., until $\xi(t)$ attains its maximum value, $r_{\rm mix}$, called mixing radius and defined by $\psi_{*\rm in}(r_{\rm mix}) = \psi_{*\rm in}(0)$; when $\xi = r_{\rm mix}$, poloidal symmetry is restored, the island O-point having evolved into the new magnetic axis, while the island X-point and the original axis annihilate each other; (ii) the time for ξ to evolve from 0 to $r_{\rm mix}$ is $\tau_K \approx (\tau_R \tau_A)^{1/2}$, with τ_A a typical Alfvén time and τ_R the global resistive diffusion time. In our model, we assume that the island growth initially follows the two basic rules of helical flux and area conservation but does not necessarily evolve to full reconnection. In addition, we do not attempt to describe the dynamical evolution; rather, the function $\xi(t)$ is inferred from the experiments.

Our problem, now, is to specify a function $\psi_*(r, \alpha; t)$ whose contour levels correspond to croissant-shaped surfaces of the type shown in region III of Fig. 2, satisfying the basic reconnection rules. These rules do not define a unique solution for the functional ψ_*, although

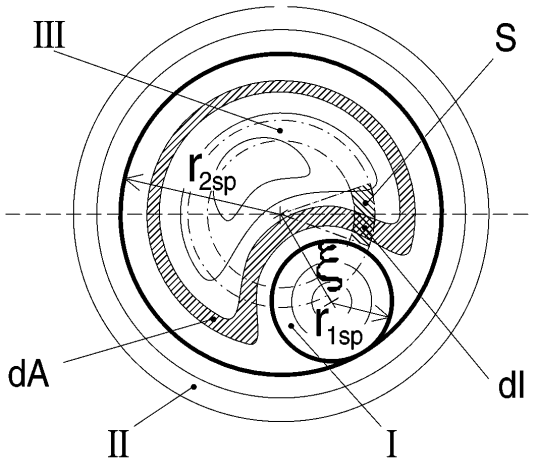

FIG. 2. Magnetic island topology; S is the heat source.

they represent a rather strong mathematical constraint. We find it convenient to introduce a Hamiltonian for the magnetic field lines inside the island separatrix (region III), $H = H(\psi_*) = H(r, \alpha; \xi)$, specifically

$$H = \frac{(r^2 + \xi^2 - 2\xi r\cos\alpha - r_{1sp}^2)(r_{2sp}^2 - r^2)}{r^2 + \xi^2 - 2\xi r\cos\alpha}, \quad (1)$$

with $\psi_{*\mathrm{in}}(r)$ and $\xi(t)$ prescribed functions. The island separatrix for a given ξ corresponds to the contour level $H = 0$, while H reaches a maximum value, $H_{\max}(\xi)$, on the island O-point. Croissant-shaped magnetic surfaces correspond to contour levels $H = H_0 \in [0, H_{\max}]$. Note that the curves $H(r, \alpha; \xi) = H_0$ become circles in both limits $\xi = 0$ and $\xi = r_{\mathrm{mix}}$ (in the latter limit, $r_{1sp} = 0$). The function $A = A(H)$ can be evaluated numerically after computing the area, A, pertaining to each $H = H_0$ surface; from this, using the area conservation rule, the function $\psi_* = \psi_*(H)$ can be easily constructed. Outside the island separatrix (regions I and II of Fig. 2) the magnetic surface cross sections are circular.

Also represented in Fig. 2 is the region where the electron heat source, S, is deposited. This region is localized on the poloidal midplane between radii r_{h1}, r_{h2}; the poloidal localization is due to focusing of the ECH wave. Taking into account plasma rotation (assumed to be rigid for the sake of simplicity), the heated region as seen in the plasma rest frame over time scales longer than τ_{rot} is in fact a ring, of volume V_h, as indicated by the dash-dotted line in Fig. 2. Thus, in the plasma frame we have $S = \rho\mathcal{H}[(r - r_{h1})(r_{h2} - r)]$, where $\mathcal{H}$ is the Heaviside function and $\rho = P/V_h$. Since parallel heat conduction is very large, the deposited heat spreads rapidly and uniformly over all flux tubes intersecting the heated ring. Thus, if we denote by dA the cross-sectional area of a generic flux tube and by dI its intersection with the heated ring (Fig. 2), we can write the ECH power density averaged over flux surfaces as $\langle S\rangle(A) = \rho\,\partial I/\partial A$. Note that the heat is transported radially by parallel heat diffusion in a complex magnetic structure, such as that of Fig. 2, resulting in an apparently nonlocal heat transport process.

Let us now discuss how the plasma density and pressure evolve during the growth of the $m/n = 1$ island. Let us disregard, for a moment, the heat source and perpendicular diffusion process. In addition, we neglect magnetic to thermal energy transfer; we have checked that this accounts for about only 1%–2% of the transferred heat. Then the area conservation rule implies the following conservation law for the plasma pressure: $\pi\int_{r_{1sp}}^{r_{2sp}} p(r^2)\,dr^2 = \int_A p(A')\,dA'$, which in differential form becomes

$$p(A) = \pi\left[p(r_{2sp}^2)\frac{dr_{2sp}^2}{dA} - p(r_{1sp}^2)\frac{dr_{1sp}^2}{dA}\right] = p(\psi_*) \quad (2)$$

since $A = A(\psi_*)$. Particle conservation yields the same relation for the plasma density. We make the simplifying (and experimentally verified [1,5]) assumption of a flat electron density. Then, since $p = nT$, Eq. (2) can be written for the temperature as well.

If we now consider the presence of the heat source and the effect of perpendicular heat diffusion, then the pressure and the temperature will depend explicitly on time: $T = T(A, t)$. In this Letter, we assume $\chi_\perp = \mathrm{const}$. This choice is made on purpose, as we wish to emphasize that, with our model, multipeaked temperature structures and sharp gradients are obtained without having to assume any specific spatial dependence for $\chi_\perp$. It is convenient to express the heat transport equation in a Lagrangian frame of reference. We also have to take into account the different topology of the three regions I, II, and III. Thus, in region III, we obtain the diffusion equation

$$\frac{3}{2}\frac{\partial T}{\partial t} = \chi_\perp\left(\langle|\nabla A|^2\rangle\frac{\partial^2 T}{\partial A^2} + \langle\nabla^2 A\rangle\frac{\partial T}{\partial A}\right) + \frac{\langle S\rangle}{n}. \quad (3)$$

Similar equations apply to regions I and II, with $A = \pi r^2$ and r the distance from the displaced axis in region I. The time evolution of the three regions is specified by the displacement function $\xi(t)$ and by $\psi_{*\mathrm{in}}(r)$, together with Eq. (1). The solution of Eq. (3) requires an initial condition, $T(r, t = 0) = T_{\mathrm{in}}(r)$, where at $t = 0$, $\xi(0) = 0$, and the following boundary conditions: a condition at the edge of the integration domain, $\tilde{r} \approx 1.5 r_{\mathrm{mix}}$, located in region II, specifically $T(\tilde{r}, t) = T_{\mathrm{in}}(\tilde{r})$; the geometrical conditions $(\partial T_{\mathrm{I}}/\partial r_1)_{r_1=0} = (\partial T_{\mathrm{III}}/\partial A)_{A=0} = 0$ on the two magnetic axes of regions I and III, respectively. Finally, a condition on the separatrix is required. Note that, with $\chi_\perp = 0$, a discontinuity of the temperature across the separatrix is in general allowed by (2). With finite $\chi_\perp$, a common temperature is achieved approaching the separatrix from any of the three regions I, II, and III, which is determined by the continuity of the heat flux. Equations (1)–(3), with the appropriate initial conditions as described above, completely specify our simulation model.

We present a typical solution obtained for the following input parameters [5]: (i) initial helical function $\psi_{*\mathrm{in}}(x) = \psi_0 x^2(1 - x^2)$, where $x \equiv r/r_{\mathrm{mix}}$; (ii) a specified displacement function, $\xi(t)$, inferred from experimental data and shown in Fig 3(a); (iii) a power source with $P = 180$ kW, $x_{h1} = 0.3$, and $x_{h2} = 0.4$; (iv) a sawtooth period $\tau_{\mathrm{saw}} = 2$ ms; (v) a value $\chi_\perp = 0.05$ m^2/s; (vi) a normalized rotation period, $\tau_{\mathrm{rot}}/\tau_{\mathrm{saw}} = 1/18$; (vii) an initial temperature profile, $T_{\mathrm{in}}(r) = T_0(1 - r^2/a^2)$, with $T_0 = 0.8$ keV. Tridimensional reconstructions of the simulated electron temperature at various phases during the growth of the $m/n = 1$ magnetic island are shown in Figs. 3(b) and 3(c). Shown in Figs. 3(d)–3(f) are examples of the simulated temperature profiles. These figures should be compared with the TEXT-U measurements in Fig. 1 (see also Figs. 10 and 11 of Ref. [5]), as well as the RTP temperature profiles in Figs. 3 and 4 of [1]. The similarities are quite evident. In particular, our model is

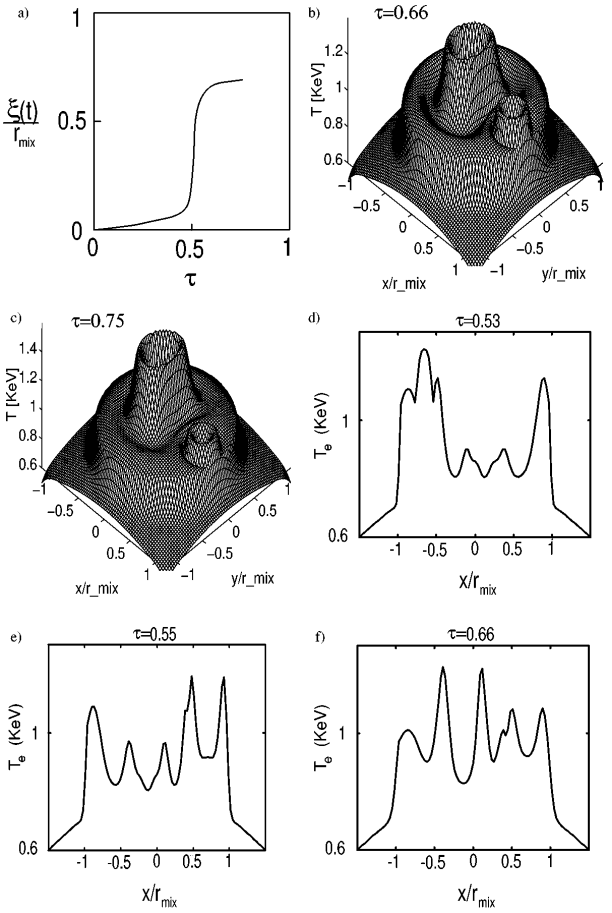

FIG. 3. Simulation results. (a) Displacement function, $\tau \equiv (t - t_0)/\tau_{\mathrm{saw}}$; (b) and (c): examples of 3D reconstructions of T_e; (d)–(f): examples of T_e profiles.

able to reproduce temperature profiles with four to five peaks, fairly independently of the precise size and localization of the heat absorption region, as long as the width of this region is small compared with the $q = 1$ radius. Once this is established, the presence of four to five peaks is fairly straightforward to comprehend. The point is that, within each of the regions I and III of Fig. 2, it is easy to form a rim structure, which shows up as two peaks per rim in the temperature profile. An additional rim is established at the island separatrix itself [compare Figs. 3(b) and 3(f)]. The outer rim structure is also quite evident from the TEXT-U experiment reconstructions shown in Figs. 1(c) and 1(d).

In addition, our model predicts the formation of sharp temperature gradients just outside the mixing radius. These sharp gradients are formed as the specific $m/n = 1$ resistive internal kink convection pattern advects the heat deposited inside the $q = 1$ radius to the separatrix region at a rate faster than the heat diffusion rate across field lines.

We can think of two possible directions for the refinement of the present model. First, one may consider a temperature-dependent diffusion coefficient. If $\chi_\perp$ were lower where the temperature is higher, the peaks in the electron temperature profile would become even sharper. Second, one may relax the single helicity assumption for the island evolution. For instance, the $m = 2$, $n = 1$ satellite harmonic for the helical flux perturbation would create a band of stochasticity in the field structure around (mostly inside) the separatrix [9]. Clearly, a fully stochastic magnetic field would not support temperature gradients. All we can say, at the moment, is that judging from the experimental data, this band of stochastic field lines should be relatively narrow during most of the sawtooth ramp.

In conclusion, we have presented a theoretical model that is able to explain the observed multipeaked temperature profiles, previously referred to as temperature filamentation [1], in ECH experiments. In addition, the model predicts the formation of sharp gradients near the sawtooth mixing radius. This transport barrier just outside the sawtooth mixing radius is a consequence of $m/n = 1$ heat convection, rather than reduced perpendicular heat diffusion near the $q = 1$ rational surface. These results are obtained even with a constant $\chi_\perp$, provided that the growth time of the $m/n = 1$ magnetic island is shorter than the cross-field heat diffusion time, and the width of the EC heated region is smaller than the $q = 1$ radius. We may expect that the sometimes observed minor structures in the electron temperature profile at rational q values can be explained along similar lines, i.e., as a consequence of macroscopic island dynamics with $m/n = q_{\mathrm{rational}}$.

The authors acknowledge useful discussions with Dr. N. J. Lopez Cardozo, Dr. A. Pochelon, and Dr. A. Pietrzyk. One of us (F. P.) was supported in part by the Italian Research Council (C.N.R.), while A. W. acknowledges the Texas Atomic Energy Research Foundation for financial support.

[1] N. J. Lopez Cardozo *et al.,* Phys. Rev. Lett. **73**, 256 (1994).
[2] M. R. de Baar *et al.,* Phys. Rev. Lett. **78**, 4573 (1997).
[3] N. J. Lopez Cardozo *et al.,* Plasma Phys. Controlled Fusion **39**, B303 (1997).
[4] S. von Goeler *et al.,* Phys. Rev. Lett. **33**, 1201 (1974).
[5] G. Cima *et al.,* Plasma Phys. Controlled Fusion **40**, 1149 (1998).
[6] V. Erckmann and U. Gasparino, Plasma Phys. Controlled Fusion **36**, 1869 (1998).
[7] B. Coppi *et al.,* Fiz. Plasmy **2**, 961 (1976) [Sov. J. Plasma Phys. **2**, 533 (1976)].
[8] B. B. Kadomtsev, Fiz. Plasmy **1**, 710 (1975) [Sov. J. Plasma Phys. **1**, 389 (1975)].
[9] A. J. Lichtenberg, Nucl. Fusion **24**, 1277 (1984).